Sea-ice floe-size distribution in the context of spontaneous scaling emergence in stochastic systems

Agnieszka Herman*
Institute of Oceanography, University of Gdańsk, 81-378 Gdynia, Poland
(Received 9 April 2010; published 28 June 2010)

Sea-ice floe-size distribution (FSD) in ice-pack covered seas influences many aspects of ocean-atmosphere interactions. However, data concerning FSD in the polar oceans are still sparse and processes shaping the observed FSD properties are poorly understood. Typically, power-law FSDs are assumed although no feasible explanation has been provided neither for this one nor for other properties of the observed distributions. Consequently, no model exists capable of predicting FSD parameters in any particular situation. Here I show that the observed FSDs can be well represented by a truncated Pareto distribution $P(x)=x^{-1-\alpha}\exp[(1-\alpha)/x]$, which is an emergent property of a certain group of multiplicative stochastic systems, described by the generalized Lotka-Volterra (GLV) equation. Building upon this recognition, a possibility of developing a simple agent-based GLV-type sea-ice model is considered. Contrary to simple power-law FSDs, GLV gives consistent estimates of the total floe perimeter, as well as floe-area distribution in agreement with observations.

DOI: 10.1103/PhysRevE.81.066123 PACS number(s): 05.65.+b, 92.10.Rw, 05.40.−a, 45.70.Vn

I. INTRODUCTION

Vast areas of the polar oceans are permanently or seasonally covered with ice pack—a mixture of ice floes with various sizes and shapes. Because of limited availability of data concerning floe-size distribution (FSD), this kind of information is typically not taken into account in studies of physical and biochemical processes in ice-covered seas—even though the size of ice floes affects many aspects of those processes. FSD influences mechanical strength of the ice and thus its response to wind and wave forcing. Due to drag-form effects, the velocity of smaller floes is usually smaller than that of larger floes, which modifies the atmosphere-ocean momentum transfer. The lateral-melting rate depends on the total perimeter of ice floes occupying a given area. For power-law FSDs, the value of the total perimeter is very sensitive to the exponent of the distribution [1]. Meanwhile, in most numerical sea-ice models even that kind of information is not available and very crude lateral-melting approximations are used [2]. FSD influences also the ocean-atmosphere heat flux and the response of the ice cover to the thermal forcing. For example, radiant and turbulent heat transfer in thin Antarctic ice depends on the ice concentration and on the width of leads between ice floes [3]. Heat-flux estimates based on ice concentration alone tend to be underestimated. On a larger scale, the structure of the ice pack may influence processes of convection and deep-water formation in polar regions. Finally, FSD affects biological processes in the ice, e.g., by modifying the amount of light and oxygen available to organisms inhabiting the surface ocean layers and the ice itself. In particular, most algae occupy the ice surface within a given distance (a few meters) from the ice edge [4].

One of the first well-documented studies concerning the ice-floe size distribution was performed by Rothrock and Thorndike [5], who analyzed satellite (Landsat) images and aerial photographs of the Arctic-ocean ice pack. The resolution and spatial coverage of their data permitted to identify floes with diameters ranging from 100 m to about 30 km. Within that range, the calculated floe sizes could be well described with a power-law distribution $P(d)\sim d^{-\alpha-1}$, with an exponent α ranging from 1.7 to 2.5 (Table I). Similarly, a good power-law fit (with $\alpha=2.16$) was obtained for an ice-floe distribution in the Sea of Okhotsk [6]. A similar study based on a photograph of the Antarctic ocean suggested two values of α (obtained with two different methods), 1.36 and 1.56, for floes smaller than 100 m [7]. A number of studies suggested that the exponent of the observed FSDs depends on the distance from the ice edge, i.e., α is largest in the marginal ice zone due to the action of waves and winds and it decreases toward the inner regions of the ice pack, where ice concentration exceeds 90% and no waves can penetrate. For example, an analysis of satellite pour l'observation de la terre (SPOT) images of an ice pack surrounding the Svalbard archipelago produced α increasing from 1.0 in the internal ice zone to 1.8 close to the ice edge [8]. A similar FSD feature (with slightly higher values of α) was observed in the Sea of Okhotsk [9].

At a laboratory scale, power-law distributions of ice pieces resulting from fragmentation of larger ice blocks were observed as well (e.g., [10–12]). In many of those studies, fragmentation of ice is analyzed with tools of fractal theory, suggesting that physical processes responsible for ice fragmentation are scale invariant. In that framework, the exponent α of the observed distributions is interpreted as a fractal dimension of these distributions. Observed values of α at a laboratory scale are generally higher than those observed at a geophysical scale [11].

Although a relatively large number of studies concerning FSD are available, no satisfactory explanation exists neither for the differences between the exponents of the observed FSDs nor for deviations from the power-law distribution exhibited by various data sets. The deviations are often attributed to limited spatial resolution and size of analyzed images. Finite-size effects typically manifest themselves in truncated power-law distributions. In short, the "curvature"

*oceagah@univ.gda.pl; http://www.ocean.univ.gda.pl/~herman/

TABLE I. Observed power-law sea-ice floe-size distributions.

Study	α	Comments
[5]	1.7–2.5	Ice floes larger than 100 m
[6]	2.16	Ice floes larger than 100 m
[8]	1.0–1.8	1.0: internal ice zone
		1.8: marginal ice zone
[7]	1.36, 1.56	Values obtained with two methods
[13]	1.8–2.9	
[14]	2.1–2.5	
[15]	2.5	
[9]	1.5–2.1	1.5: internal ice zone
		2.1: marginal ice zone
[1]	1.15–1.87	α larger for larger floes
[16]	1.83–2.36	Floe width 20–50 m
	0.91–0.94	Floe width 2–20 m

of FSDs in log-log plots [1,5,8] is often interpreted as a feature attributable to the data collection and analysis methods and not to a really existing property of the ice pack itself. Only recently, the existence of (a) physical process(es) responsible for the change in α between small and large floes has been suggested by Toyota and colleagues [1]. In their study, they combined ship-borne, helicopter-borne, and Landsat images to cover a broad range of scales from below 1 m to over 1 km. Hence, the change in slope of the FSD in their data can be hardly attributed to insufficient resolution of the images used to obtain this FSD. Similarly, Steer and colleagues [16] photographed the ice pack in the western Weddell Sea as part of the Ice Station Polarstern (ISPOL) experiment [17]. They also observed the change in slope of the FSD. However, contrary to how the above authors interpret their results [1,16], in both cases the change in slope of the FSD seems rather gradual than abrupt. Instead of a combination of two power laws "glued together" at a highly arbitrarily chosen floe diameter, another type of distribution would be desirable. It should reflect the observed gradually increasing deviation from a power-law distribution for decreasing floe diameter.

Here, I postulate that the distribution of scaled ice-floe diameters is well characterized with a function:

$$P(x) = x^{-1-\alpha} \exp[(1-\alpha)/x]. \tag{1}$$

Suitability of Eq. (1) for describing the observed FSDs is demonstrated for the ISPOL data of [16] in Sec. II. In Sec. II B, the resulting floe-area distribution (FAD) is analyzed. Properties of this FSD are discussed in Sec. II C. Finally, in view of the fact that distribution (1) is an emergent property of a GLV equation, in Sec. III basics of agent-based models, properties of GLV models and possibilities of formulating a GLV model for floe–floe interactions are discussed.

Distribution (1) will be further called a GLV distribution.

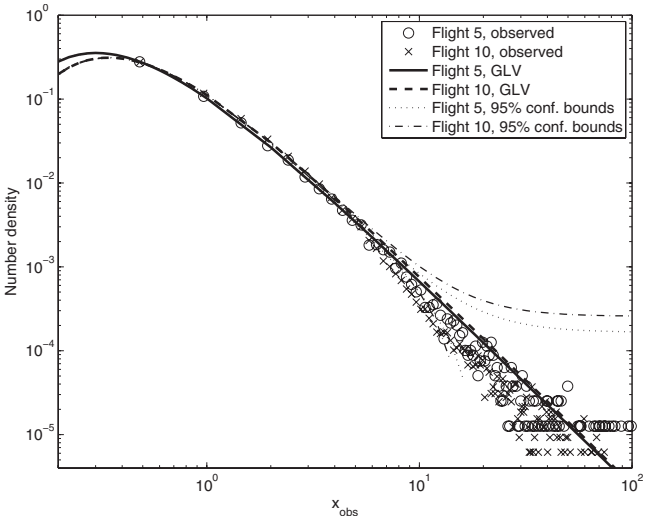

FIG. 1. Distribution of the scaled floe diameters $x_{i,\mathrm{obs}}$ during ISPOL flights 5 and 10.

II. GLV FIT TO THE ISPOL DATA

A. Floe-size distribution

The ISPOL experiment was an interdisciplinary study of physical and biogeochemical ocean-ice-atmosphere interactions in the western Weddell Sea ([17] and references therein). As part of the experiment, Steer and colleagues [16] used aerial photographs of the ice cover (with resolution of $\sim$0.4 m), collected during seven flights, for an analysis of the temporal changes of FSD and FAD during the melting season in the western Weddell Sea. Two of the flights, flights 5 and 10, were reported in the paper and are analyzed here.

Let us consider a given sea area covered with ice floes. The floes have different effective diameters, defined as square roots of their surface areas. The average diameter of these floes equals $\bar{d}$. Due to the limited resolution of the images and/or finite-area effects and/or limitations of the technique used to identify floe boundaries in the images, only a subset of N floes can be analyzed. We denote effective diameters of these floes with d_i $(i=1,\ldots,N)$ and their average with $\bar{d}_{\mathrm{obs}}$. For the scaled floe diameters x_i we have

$$x_i \equiv \frac{d_i}{\bar{d}} = \frac{d_i}{\bar{d}_{\mathrm{obs}}}\frac{\bar{d}_{\mathrm{obs}}}{\bar{d}} = x_{i,\mathrm{obs}}\frac{\bar{d}_{\mathrm{obs}}}{\bar{d}} = x_{i,\mathrm{obs}}c^{-1}. \tag{2}$$

If x_i are distributed according to Eq. (1), then for the "observed" scaled floe diameters $x_{i,\mathrm{obs}}$:

$$P(x_{\mathrm{obs}}) = \tilde{c}x_{\mathrm{obs}}^{-1-\alpha} \exp[c(1-\alpha)/x_{\mathrm{obs}}]. \tag{3}$$

The ratio of the real to the observed average diameters c is not known *a priori* and must be estimated together with α and the scaling constant $\tilde{c}$ during the fitting process.

The results of the least-squares fit for flights 5 and 10 are shown in Fig. 1 and in Table II. For both flights $c>1$ $(\bar{d}>\bar{d}_{\mathrm{obs}})$, which is not surprising as only floes that entirely lied within the images were taken into account, i.e., the largest floes were omitted in the analysis. The values of α for both flights fall in between the two values obtained with a

TABLE II. Results of the least-squares fit of the GLV distribution $P(x_{i,\mathrm{obs}})$ to the ISPOL flights 5 and 10 data.

	N	$\bar{d}_{\mathrm{obs}}$	α	c	α_{obs}	RMSE	r^2
Flight 5	79357	4.34	1.477 ± 0.009	1.562 ± 0.016	1.745	0.84×10^{-4}	1.0000
Flight 10	324044	3.94	1.509 ± 0.013	1.702 ± 0.023	1.866	1.31×10^{-4}	0.9999

power-law fit [16]. The fitted distributions pass directly through the data points for $x<5$, but considering the increasing scatter of the data with increasing x, the fit can be regarded as satisfactory in the whole data range, especially if one considers that the larger the floe diameter, the lower the probability of observing it within an image, so that the tails of the observed FSDs tend to be underestimated.

B. Floe-area distribution

The FAD is directly related to the distribution of effective floe diameters, which by definition are proportional to the square root of floe areas. Steer and colleagues [16] propose a negative-exponential fit to the observed FAD. But how this kind of FAD could result from a power-law distribution of floe diameters? The two function types proposed for FSD and FAD are not consistent with each other. Here, given the observed floe-size distribution [Eq. (3)], the corresponding FAD is

$$P_a(x_{\mathrm{obs}}) = \tilde{c} x_{\mathrm{obs}}^{1-\alpha} \exp[c(1-\alpha)/x_{\mathrm{obs}}]. \tag{4}$$

Figure 2 shows the results of the least-squares fit of $P_a(x)$ to the observed FADs for flights 5 and 10. The scatter of data is higher than in the case of the FSD. Nevertheless, most data points, including those representing the largest floes, lie within the 95% confidence interval from the fitted lines. Importantly, $r^2>0.9$ for floes with diameters smaller than ~40 m ($x_{\mathrm{obs}}<10$) and for larger floes the calculated distribution passes through the middle of the data "cloud." The negative-exponential fit is definitely inadequate for the large-floe part of the observed distributions [16]. Interestingly, maximum of P_a occurs for $x=1$ independently on α, i.e., the average-size floes are not the most frequently occurring ones, but occupy the largest fraction of the total ice-covered area.

C. Properties of the GLV distribution

Contrary to most distribution functions proposed for FSDs, Eq. (1) has a maximum at

$$x_{\max} = (\alpha-1)/(\alpha+1) \quad \text{or} \quad x_{\max,\mathrm{obs}} = c x_{\max}. \tag{5}$$

Thus, $x_{\max,\mathrm{obs}}=0.30$ ($d_{\max}=1.30$ m) and $x_{\max,\mathrm{obs}}=0.34$ ($d_{\max}=1.34$ m) for flights 5 and 10, respectively (Fig. 1). Unfortunately, in the case of the ISPOL data, maxima of the fitted distributions lie outside of the observed range of floe sizes. But, remarkably, the observed FADs do have maxima (Fig. 2), which they would not have if the corresponding FSDs were of the power-law type with $\alpha>1$. The maxima given by the GLV distributions correspond well with the observed ones (Fig. 2).

Does a physical mechanism exist that favors a dominating floe size? It is known that when smaller floes break, the characteristic size of pieces depends on the length of elastic waves in the ice [18]. In typical conditions, this size varies between 15–30 m for ice thickness 1–3 m. These values are much larger than $d_{\max}$ resulting from the GLV fit to the

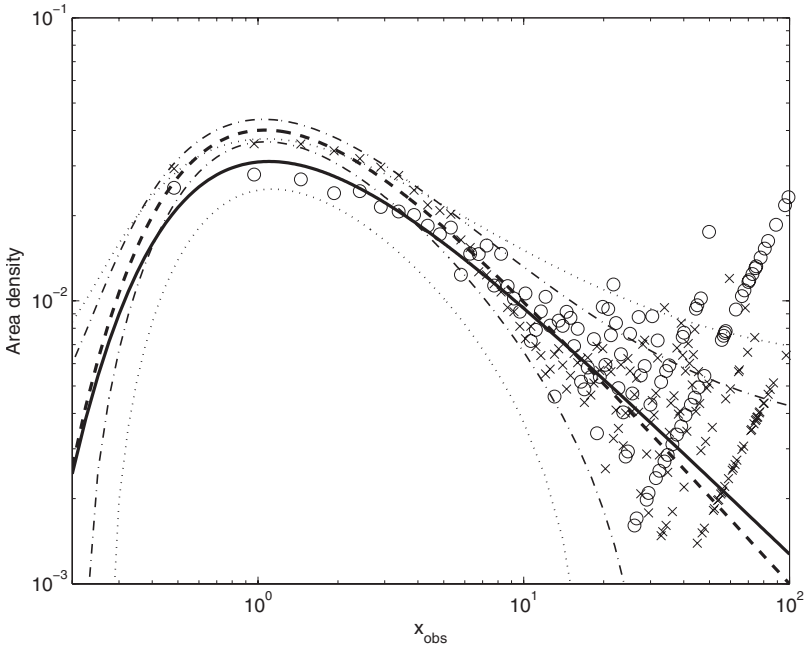

FIG. 2. Floe-area distribution of the scaled floe diameters $x_{i,\mathrm{obs}}$ during ISPOL flights 5 and 10. For legend, see Fig. 1.

ISPOL data. Also, no maxima occur in this floe-size range in the observed data. Hence, in the analyzed case breaking due to elastic waves cannot be responsible for the properties of the FSD. Actually, the obtained $d_{\max}$ is comparable to the thickness of first-year ice floes in the study area [19] and, as it is hard to imagine floes with vertical dimension larger than horizontal dimension, maybe this simple explanation is sufficient to explain that the FSD decreases rapidly for x corresponding to floes with size comparable to and smaller than the ice thickness.

Another striking feature of the GLV distribution is that the same parameter α occurs in its exponential and power-law parts. Thus, it links the distribution of the lowest values of x (described by the exponential part) with the distribution of the largest values of x (where the power-law part plays a dominating role). This feature is particularly interesting in the context of the GLV model discussed further.

III. DISCUSSION AND CONCLUSIONS

A. Generalized Lotka-Volterra model

With the above-described FSD properties in mind, I turn to an agent-based approach in order to investigate the possibility of developing a simple model of interactions among a population of ice floes. The term "population" is borrowed from ecology and population-dynamics research, in which—similarly as in economy and social sciences—agent-based modeling (ABM) (equivalently: individual-based modeling) has recently become a widely used and recognized tool. Generally, ABMs are used to simulate the dynamics of populations of a large number of similar elements (agents), interacting at the microscopic individual level. Collective behavior of agents results in emergent properties of the analyzed population, i.e., macroscopic properties that cannot be directly deduced from individual-level laws. The ABM considered here is based on a GLV model, applicable for populations of autocatalytic, competing elements. GLV is an extension of the Lotka-Volterra model (e.g., [20]) and has been used in a number of studies in the context of economy and population dynamics [21–24].

Let d_i $(i=1,\ldots,N)$ denote the value of a certain property of the ith of N analyzed agents. According to GLV, the change in d_is between time t and $t+\tau$ is given by

$$d_i(t+\tau) = [1 + \lambda_i(t) - c(\mathbf{d},t)]d_i(t) + \hat{a}(\mathbf{d},t), \tag{6}$$

$$d_j(t+\tau) = d_j(t), \quad j = 1,\ldots,N, \quad j \neq i. \tag{7}$$

The update mechanism is asynchronous and i is chosen randomly at each time step τ (which must be much smaller than the rate of change in the forcing). In Eq. (6), $\mathbf{d}=(d_1,\ldots,d_N)$, $\lambda_i(t)$ denotes a random variable drawn from a prescribed distribution $\Pi(\lambda,t)$; $\lambda_i(t)$ is a sum of a constant (or slowly varying) and a random part: $\lambda_i(t)=\langle\lambda\rangle+\eta_i(t)$, with $\langle\eta\rangle=0$ and $\langle\eta^2\rangle=D$ (where $\langle\cdot\rangle$ denotes time averaging). Functions $\hat{a}$ and c are slowly varying, positive, and $\hat{a}$ is symmetrical with respect to the first N arguments.

In most GLV models, $\hat{a}(\mathbf{d},t)=a(t)\bar{d}$. In that case, if we define $\bar{d}=\Sigma_{i=1}^{N} d_i/N$ and scaled variables $x_i=d_i/\bar{d}$, then [24]

$$x_i(t+\tau) = [1 + \eta_i(t)]x_i(t) + a(t)\bar{d}[1 - x_i(t)], \tag{8}$$

which is equivalent to a discrete-time Langevin equation known from statistical physics. The distribution of x_i is given by Eq. (1) with

$$\alpha = 1 + 2a/D, \tag{9}$$

i.e., α does not depend neither on c nor on λ and therefore remains relatively stable even in rapidly changing environment conditions. The average $\bar{d}$ can also vary without affecting α. GLV simulations result in populations exhibiting Lévy-stable fluctuations around a (slowly varying) equilibrium value [25,26]. It is an example of a so-called spontaneous scaling emergence in stochastic systems [27,28].

B. Floe-floe interactions from a GLV perspective

Is the GLV model suitable for describing interactions between ice floes? In other words, is it possible to assign processes influencing FSD to the three basic terms in Eq. (6)? Formulating precise expressions for λ, $\hat{a}$, and c is beyond the scope of this paper, but it is tempting to make some preliminary considerations on that matter.

Typically, the ice pack consists of thick multiyear ice floes and thinner first-year ice occupying the cracks and leads between them (e.g., during ISPOL, the ice thickness distribution had two distinct peaks representing those two ice types [19]). In the model discussed here, it seems reasonable to define the agents as thick floes surrounded by open water and other ice types that may influence the behavior and interactions between the proper floes but are not modeled themselves.

Let us consider a population of N ice floes with surface areas $s_1,\ldots,s_N$ and effective diameters $d_i=s_i^{1/2}$. The (variable) sea-surface area available to the floes equals S and the ice concentration in S is $A=S^{-1}\Sigma_{i=1}^{N} d_i^2$. Obviously, $A \leq 1$, which poses a limitation on the growth of the ice floes and (in the ABM terminology) introduces competition for limited resources (the available surface area). Preliminary simulations with a GLV model showed that if $c(d_1,\ldots,d_N,t)=A(t)$, the modeled d_is can be effectively kept within the desired limit. Depending on the external conditions (wind, tides, waves, and ocean-ice-atmosphere heat flux) and on the concentration and properties of the ice floes themselves, they may break apart, freeze together, collide with neighbors, melt, and so on. At least for some of these processes, mathematical formulations exist that could be assigned to the terms in Eq. (6). For example, nonuniform motion of neighboring floes leads to compressive, tensile, and shear stresses in the ice, which are proportional to the velocity differences at both ends of a floe, and thus proportional to its size [29–31]. Thus, breaking probability is larger for larger floes and it could be represented by the $\lambda_i(t)d_i(t)$ term.

C. Conclusions

Generally, data allowing us to estimate temporal changes of FSD in relation to external forcing would be necessary to verify the above ideas. Although the possibility of formulat-

ing a GLV-based floe-floe interaction model remains open, distribution (1) fits remarkably well to FSDs observed during ISPOL and can be used as a function representing these FSDs.

Even without a working GLV model, a number of useful parameters characterizing the ice pack can be estimated based on the proposed distribution. For example, given ice concentration A, sea-surface area S (e.g., a grid cell of a numerical model), and realistic estimates of the mean effective floe diameter $\bar{d}$ and the distribution parameter α, the total perimeter P of the (circular) floes in S equals $P = P_0(\alpha)AS/\bar{d}$ with

$$P_0(\alpha) = 2\sqrt{\pi}\frac{\int_0^\infty x^{-\alpha}\exp[(1-\alpha)/x]dx}{\int_0^\infty x^{1-\alpha}\exp[(1-\alpha)/x]dx}. \quad (10)$$

Function P_0 increases with increasing α and it is finite for $\alpha > 1$. Whereas power-law distributions lead to problems with infinite surface areas and total floe perimeters [5], GLV gives physically feasible results in this respect, which provides another argument for its usage.

The estimate [Eq. (10)] could be further improved if α were calculated from the external forcing, as in Eq. (8). Nevertheless, P and other FSD-dependent parameters could be used in numerical sea-ice models, e.g., in improved lateral melting algorithms.

ACKNOWLEDGMENTS

I would like to thank Professor Sorin Solomon from the Hebrew University in Jerusalem, Israel, who had a deciding influence on the research presented in this paper. I am also grateful to Adam Steer from the Australian Antarctic Division in Kingston, Tasmania, for providing me the ISPOL data and all related information necessary to conduct this study.

[1] T. Toyota, S. Takatsuji, and M. Nakayama, Geophys. Res. Lett. **33**, L02616 (2006).
[2] M. Steele, J. Geophys. Res. **97**, 17729 (1992).
[3] A. Worby and I. Allison, Ann. Glaciol. **15**, 184 (1991).
[4] M. Grose and A. McMinn, in *Antarctic Biology in a Global Context*, edited by A. H. L. Huiskes *et al.* (Backhuys, Leiden, Netherlands, 2003), Vol. 21.
[5] D. Rothrock and A. Thorndike, J. Geophys. Res. **89**, 6477 (1984).
[6] M. Matsushita, J. Phys. Soc. Jpn. **54**, 857 (1985).
[7] M. Lensu, in *Proceedings of IAHR Ice Symposium*, Espoo, Finland (Helsinki University of Technology, Helsinki, 1990) pp. 300–313.
[8] C. Kergomard, Bull. de la SFPT **115**, 17 (1989).
[9] J. Inoue, M. Wakatsuchi, and Y. Fujiyoshi, Geophys. Res. Lett. **31**, L20303 (2004).
[10] J. Weiss and M. Gay, J. Geophys. Res. **103**, 24005 (1998).
[11] J. Weiss, Eng. Fract. Mech. **68**, 1975 (2001).
[12] Y. Xu, J. Xu, and J. Wang, Cold Regions Sci. Technol. **40**, 135 (2004).
[13] B. Holt and S. Martin, J. Geophys. Res. **106**, 1017 (2001).
[14] T. Toyota and H. Enomoto, *16th International Symposium on Ice* (International Association for Hydraulic Research, Dunedin, 2002).
[15] J. Weiss, Surv. Geophys. **24**, 185 (2003).
[16] A. Steer, A. Worby, and P. Heil, Deep-Sea Res., Part II **55**, 933 (2008).
[17] H. Hellmer, M. Schröder, C. Haas, G. Dieckmann, and M. Spindler, Deep-Sea Res., Part II **55**, 913 (2008).
[18] M. Leppäranta, *The Drift of Sea Ice* (Springer-Verlag, Berlin, 2005) p. 267.
[19] C. Haas, M. Nicolaus, S. Willmes, A. Worby, and D. Flinspach, Deep-Sea Res., Part II **55**, 963 (2008).
[20] M. Nowak, *Evolutionary Dynamics: Exploring the Equations of Life* (Belknap Press of Harvard University Press, Cambridge, 2006).
[21] S. Solomon, in *Applications of Simulation to Social Sciences*, edited by G. Ballot and G. Weisbuch (Hermes Science, Oxford, 2000).
[22] S. Solomon and P. Richmond, Physica A **299**, 188 (2001).
[23] S. Solomon and P. Richmond, Eur. Phys. J. B **27**, 257 (2002).
[24] O. Malcai, O. Biham, P. Richmond, and S. Solomon, Phys. Rev. E **66**, 031102 (2002).
[25] O. Biham, O. Malcai, M. Levy, and S. Solomon, Phys. Rev. E **58**, 1352 (1998).
[26] O. Malcai, O. Biham, and S. Solomon, Phys. Rev. E **60**, 1299 (1999).
[27] M. Levy and S. Solomon, Int. J. Mod. Phys. C **7**, 595 (1996).
[28] S. Solomon and M. Levy, Int. J. Mod. Phys. C **7**, 745 (1996).
[29] M. Hopkins, J. Geophys. Res. **101**, 18315 (1996).
[30] M. Hopkins, S. Frankenstein, and A. Thorndike, J. Geophys. Res. **109**, C01032 (2004).
[31] M. Hopkins and A. Thorndike, J. Geophys. Res. **111**, C11S23 (2006).